Selection of DNA Aptamers for Differentiation of Human Adipose-Derived Mesenchymal Stem Cells from Fibroblasts

Mariane Izabella Abreu de Melo (abreu.mariane@gmail.com)
Centro de Desenvolvimento da Tecnologia Nuclear https://orcid.org/0000-0001-7150-9435
Pricila da Silva Cunha
Centro de Desenvolvimento da Tecnologia Nuclear
Marcelo Coutinho de Miranda
Universidade Federal de Minas Gerais
Joana Lobato Barbosa
Universidade Federal de Minas Gerais
Jerusa Araújo Quintão Arantes Faria
Universidade Federal do Amazonas
Michele Angela Rodrigues
Universidade Federal de Minas Gerais
Alfredo Miranda de Goes
Universidade Federal de Minas Gerais
Dawidson Assis Gomes
Universidade Federal de Minas Gerais

Research Article

Keywords: DNA aptamers, Cell-SELEX, human adipose-derived stem cells, human dermal fibroblasts, quantitative PCR assay

Posted Date: March 31st, 2021

DOI: https://doi.org/10.21203/rs.3.rs-287027/v1

Version of Record: A version of this preprint was published at Applied Biochemistry and Biotechnology on August 6th, 2021. See the published version at https://doi.org/10.1007/s12010-021-03618-5.

Abstract

In recent years, stem cell therapy has shown promise in regenerative medicine. In this context, the distinction of mesenchymal stem cells from fibroblasts has been crucial for safe clinical application of these cells. In the present study, we developed aptamers capable of specifically recognize mesenchymal stem cells derived from adipose tissue (ASC) using the Cell-SELEX technique. We tested the affinity of ASC aptamers compared to dermal fibroblasts (FIB). Quantitative PCR was advantageous for the validation of four candidate aptamers *in vitro*. The binding capabilities of Apta 2 and Apta 42 could not distinguish both cell types, while Apta 21 and Apta 99 showed a better binding capacity to ASC with dissociation constants (Kd) of 50.46 ± 2.28 nM and 72.71 ± 10.3 nM, respectively. However, Apta 21 showed a Kd of 86.78 ± 9.14 nM when incubated with FIB. Therefore, only Apta 99 showed specificity to detect ASC. This aptamer is a promising tool for the *in vitro* identification of ASC. These results will help understand the differences between these two cell types for more specific and precise cell therapies.

1. Introduction

Nucleic acid aptamers can be defined as single-stranded DNA or RNA oligonucleotides, generally smaller than 100-mer, capable of binding to a wide variety of target molecules with high affinity and specificity [1]. During aptamers selection, a set of random sequences is enriched by generating target-specific sequences by an *in vitro* and an iterative process called Systematic Evolution of Ligands by Exponential Enrichment (SELEX) [2, 3]. Once the target molecules are anchored to the cell surface, the bound aptamers can be easily separated from unbound oligonucleotides by washing and centrifugation during the Cell-SELEX process. This method supports the development of *in vitro* probes and the discovery of cell biomarkers [1, 4].

The mesenchymal stem cells can differentiate into distinct cell types of cells and have been isolated from the stromal fraction of practically all body tissues. Adipose tissue is an accessible source that provides higher yields of stem cells than bone-marrow [5]. These human adipose-derived stem cells (ASC) are promising self-renewing and multipotent mesenchymal stem cells. They have shown strong immunosuppressive effects and regenerative actions *in vivo*, features needed to develop novel cell-based therapy and tissue engineering strategies [6]. However, in the therapeutic application of stem cells, there is a high risk of contamination with fibroblasts (FIB), which can lead to a series of losses for the therapy, such as the decrease in the stem cell differentiation capacity and the induction of senescence [7–9].

Aiming the identification of ASC as mesenchymal stem/stromal cells, the International Society for Cell Therapy (ISCT) provided a set of criteria, such as plastic adherence, colony formation capacity, tri-lineage differentiation potential, the presence of mesenchymal, and the absence of hematopoietic cell surface markers [10]. Like ASC, FIB are plastic-adherent spindle-shaped cells. These cells can be found in the stromal portion of several tissues, such as skin, adipose and cardiac tissue, and muscle, showing an essential role in tissue development and wound healing. Both cells have an elongated, spindle-like morphology, making them indistinguishable [11, 12]. Moreover, the cell surface proteins of FIB are very similar to the profile observed in ASC [12–15].

In the context of cell therapy, for better preparation of ASC without fibroblasts, it is necessary to find markers that differentiate ASC from FIB without impairing its application condition. Thus, considering the high specificity and affinity of aptamers for their targets, we aimed to select novel aptamers after ASC (positive) and FIB (negative) selection pressures using Cell-SELEX and quantitative PCR techniques.

2. Materials And Methods

2.1 Isolation and Cell Culture

Human skin and adipose tissue were freely provided by healthy donors that underwent liposuction and abdominoplasty, according to the guidelines of Universidade Federal de Minas Gerais Research Ethics Committee (Number: 02508018.1.0000.5149).
Human ASC and FIB were isolated using mechanical and enzymatic digestion as previously described by our group [16]. Cells were cultured in Dulbecco's modified Eagle's medium (DMEM, Thermo Fisher Scientific, MA, USA) supplemented with 5 mmol/L of sodium bicarbonate (Sigma-Aldrich, MO, USA), 1% of PSA solution (penicillin/streptomycin/amphotericin B; Sigma-Aldrich) and 10% of fetal bovine serum (FBS). The cells were kept in a humidified incubator at 37°C and 5% CO_2. The medium was changed three times a week, and cells at 4th and 5th passages were used in the experiments.

2.2 Design of Oligonucleotides

The forward (5′-ATGGTCTCACTGCGTTCA-3') and the reverse (5'- AGATTCGGTAGCACAGGA-3') primers were used in the Cell-SELEX process. The reverse primer was labeled at the 5' end with biotin to allow single strand separation during Cell-SELEX. The ssDNA library comprised a randomized region of 60 nucleotides flanked by two constant primer annealing sequences: 5′-ATGGTCTCACTGCGTTCA-60N-TCCTGTGCTACCGAATCT-3'. The 65-mer scrambled sequence has the same primer hybridization region as the candidate aptamers: 5′-ATGGTCTCACATTTGGCAGGGCCTTAAGGCCATGGGCCTTAAGGCCCTCCTGTGCTACCGAATCT-3'. Based on the qPCR reaction normalization method developed by Graziani and colleagues [17], an exogenous nucleotide sequence extracted from the genome of *Arabdopshis thaliana* (AT1) was synthesized (5'-GCATGTTTGAACAGACACTGTATCTGTATTGTTACAATGGATATTGATTTGGTGTTTGCAGGATCCTGGACAGAAGCAAAGGCA-3') and the primers AT1 forward 5′-GCATGTTTGAACAGACACTG-3' and AT1 reverse 5′-TGCCTTTGCTTCTGTCCAGG-3' were used for PCR amplification. All oligonucleotides were synthesized by Integrated DNA Technologies (IDT, IA, USA).

2.3 Cell-SELEX procedure

Aptamers selection was carried out based on the Cell-SELEX protocol [1], with modifications. Previously, 2 nmol of ssDNA were diluted in binding buffer (25 mM of glucose, 0.05 mM of $MgCl_2$, 15 mM of BSA, 4 µM of yeast tRNA in 100 mL of phosphate-buffered saline solution (PBS pH 7.4; Sigma-Aldrich),

heated at 95°C for 5 minutes and snap cooled on ice before binding. Then, the ssDNA library was incubated with 3.5×10^6 in one dish (100 mm × 20 mm) for 1.5 h at room temperature. After incubation, the supernatant was discarded, and cells were washed with washing buffer (25 mM of glucose, 0.05mM of $MgCl_2$ in 1L of PBS; Sigma-Aldrich). Subsequently, cells with bound aptamers (ligands) were removed using a cell scraper and nuclease-free water. To separate cell-ligands complex, the mixture was heated to 95ºC and, subsequently, centrifuged at 13,100*×g* for 5 minutes. The optimal number of PCR cycles for each selection round was determined according to the literature [1]. After the first round of positive selection, recovered sequences were submitted to six cycles of amplification. The pool of ssDNA was amplified using 5× Colorless Buffer GoTaq® Flexi Buffer (Promega, WI, USA), 2.5 mM of each dNTP (dATP, dCTP, dGTP, dTPP), 50 mM of $MgCl_2$, 0.5 µM of primers (R labeled with biotin) and 5 U/µL of GoTaq® DNA Polymerase (Promega). The amplification conditions were: initial stage at 95°C for 3 minutes, followed by 10 cycles of 95°C for 30 seconds, 53.3°C for 30 seconds and 72°C for 30 seconds. The final extension step was performed at 72°C for 5 minutes. The double-strand DNA (dsDNA) was separated using Magnesphere® Paramagnetic Particles kit (Promega), according to the manufacturer's instructions. In the second round of incubation with ASC, the recovered ssDNA were submitted to 12 amplification cycles. In the third round of selection, the negative selection was introduced: 3×10^6 FIB cells were seeded in one cell dish. The ssDNA ligands obtained from the second round were incubated with fibroblasts for 1 hour. After this period, the supernatant containing the aptamers that did not bind to the fibroblasts was extracted, heated and centrifuged for PCR cycle test. The optimal number of 20 PCR cycles was chosen, repeated in the subsequent negative selection cycles. After amplification and separation of the double-stranded DNA, the ligands were incubated with the target cell for 1 h. The number of 16 PCR cycles was defined as the optimal cycle number, which was also used in subsequent positive selection rounds. From the 4th round on, modifications such as cell density and incubation time were introduced in the selection **(**Table 1**).** These alterations aimed to raise the stringency of the Cell-SELEX procedure until the final 8th round. The enriched aptamers of the 7th and 8th round after incubation with ASC and the ligands extracted after the incubation with FIB in the 8th round were sequenced using Illumina MiSeq platform (Illumina Inc., CA, USA). Sequencing and bioinformatics analysis were performed by GenXPro GmbH (Frankfurt am Main, Germany).

Table 1
Parameters of DNA aptamers selection

Rounds	Positive Selection: ASC	*Dish* number	Time of Incubation	PCR Cycles	Negative Selection: FIB	Time of Incubation	*Dish* number	PCR Cycles
1	$3{,}5\times10^6$	1	1h30min	6	-		-	-
2	$3{,}5\times10^6$	1	1h30min	12	-		-	-
3	3×10^6	1	1h	16	3×10^6	30min	1	20
4	3×10^6	1	45min	16	3×10^6	30min	1	20
5	5×10^5	1	30min	16	3×10^6	30min	1	20
6	5×10^5	1	30min	16	3×10^6	30min	1	20
7	5×10^5	1	30min	16	3×10^6	30min	1	20
8	5×10^5	1	20 min	16	3×10^6	20 min	2	20

2.4 Melting Curve analysis

The progress of aptamers selection was monitored by analyzing the dissociation curve (DNA melt) of ligands after each round as previously described [18, 19]. For this purpose, 5 µL of SYBR® Green PCR Master Mix 2x reagent (Applied Biosystems, CA, USA) was added to 5 µL of the PCR products containing the ligands. The samples were subjected to gradual denaturation according to the protocol: 95ºC for 15 minutes, 95ºC for 15 seconds, denaturation ramp from 40ºC to 95ºC and 25ºC for 15 seconds. Reactions were performed on the 7500 Fast Real-Time PCR System (Applied Biosystems). The graphs of fluorescence intensity versus temperature were generated on the 7.500 Software v. 2.0.6 (Applied Biosystems).

2.5 Selection and Characterization of Candidate Aptamers

Post-sequencing analyzes were performed using the Galaxy server available at https://usegalaxy.org/ [20]. The following criteria were established for the selection of candidate aptamers: (a) The more prevalent sequence in ASC compared to FIB and enriched from the 7th to the 8th round; (b) Sequences with specific affinity to ASC and enriched from the 7th to the 8th round; (c) Sequences with the lowest value of ΔG at 25°C. The secondary structures and Gibbs free energy (ΔG) of aptamers were determined using the mfold web server available at http://unafold.rna.albany.edu28, under 25ºC condition. The four aptamers were synthesized by IDT for *in vitro* validation assays.

2.6 *In Vitro* Binding Assays of Aptamers and Scramble

The four candidate aptamers and the scrambled sequence were tested for the binding capacity to human cells. ASC and FIB were plated in 6-well plates at a density of 5×10^5 cells/well and maintained in a CO_2 incubator for 24 h. The next day, 250 nM aptamers or scrambled sequences were heated to 95°C and cooled on ice for the three-dimensional structure formation. Then, they were incubated with cells for 20 minutes at room temperature under gentle agitation. Next, the cells were washed three times with cold PBS to remove unbound sequences. To recover the cell-aptamer complex, cells were removed using a cell scraper, and sequences were eluted in nuclease-free water under heating at 95°C for 10 minutes. The AT1 sequence (100 fM) was added and the samples

were centrifuged for 5 minutes at 13,200×*g*. The supernatants containing aptamers were recovered and amplified using the Go Taq® qPCR Master Mix Kit (Promega), in a CFX Touch™ Real-Time PCR Detection System (Bio-Rad Laboratories, CA, USA).

The following PCR conditions were used in all reactions: 95°C for 2 minutes, followed by 40 cycles of: 95°C for 15 seconds and a single stage of hybridization and extension at 60°C for 1 minute.
After 40 cycles of amplification, all samples were subjected to gradual denaturation. Reactions were normalized by the AT1 amplification as an internal reference control. Two different reaction mixes for each sequence were prepared: one mix in which the sequences were amplified with the original pair of primers and another mix with the pair of primers for AT1 sequence. The efficiency of each reaction was calculated based on the method described by Liu & Saint [21] and Cikos and colleagues [22]. The relative quantification was calculated using the method developed by Pfaffl [23], with Pair Wise Fixed Reallocation Randomization Test and FIB as the reference condition.

2.7 Determination of Aptamers Dissociation Constant

The Kd value of each candidate aptamers were estimated using the non-linear regression curve as previously described by our group [24]. ASC and FIB were plated at a density of 2.5×10^5 cells per well in 12-well plates and maintained in a CO_2 incubator for 24 h. The next day, cells were incubated with different concentrations of each aptamer for 20 minutes at room temperature under gentle agitation. After incubation, the cell-aptamer complex was extracted with nuclease-free water and a cell scraper. Bound aptamers were recovered by heating the complex at 95°C and subsequent centrifugation for 5 min at 13,200×*g*. The supernatant was collected and amplified by qPCR using GoTaq® qPCR Master Mix Kit (Promega). The reaction mixture contained 5 µL of GoTaq® qPCR Master Mix (2X), 0.2 µM of each primer, 4 µL of aptamers samples and 0.6 µL of nuclease-free water. The amplification steps were initial heating of 95°C for 2 min followed by 40 cycles of 95°C for 15 s and 60°C for 1 min. After amplification, samples were subjected to gradual denaturation to determine the melting curve using CFX Touch™ Real-Time PCR Detection System (Bio-Rad Laboratories). Standard curves for each pure aptamer were generated and the correspondent equations were used in the conversion of Ct values from bound aptamers to nanograms. After obtaining these values, a saturation curve was plotted (cell bounded aptamers in nanograms vs the aptamer concentration used in the incubation). The Kd was determined using non-linear regression in GraphPad Prism 7 software (Graph-Pad Software Inc., La Jolla, CA, USA).

2.8 Statistical Analysis

Data were expressed graphically as mean ± standard deviation (SD). Normal distribution was verified using the D'Agostino & Pearson normality test. Unpaired t-test with Welch's correction was used to compare pairs of means. The non-linear regression equation (Specific Binding with Hill Slope) was used to determine Kd values. Statistical significance was considered when $p < 0.05$. All statistical analyzes were performed using GraphPad Prism 7 software.

3. Results And Discussion

Cell-SELEX was performed to select aptamers that specifically bind to ASC, with negative selection steps using human FIB. Due to the similarity of the surface markers (CD) between ASC and FIB, the search for a marker to selectively differentiate these two cell types becomes of great interest. We monitored the progression of the aptamers selection by DNA melt assay, an informative method for rapid qualitative evaluation of the aptamers pool's diversity [18, 19]. Aptamers melting profiles in all selection rounds are shown in Supplementary Information **(Fig. S1).** The aptamers, corresponding to the 7th round of selection in ASC and the 8th round of selection in ASC and FIB, were sequenced and analyzed by bioinformatics to select candidate aptamers for *in vitro* validation. Based on the criteria established, four candidate nucleotide sequences were selected and named based on their position in the 8th round of positive selection **(**Table 2**).**

Table 2
Nucleotide sequences of the candidate aptamers selected for *in vitro* validation.

Aptamer	Nucleotide Sequence
Aptamer 2 (Apta 2)	5'ATGGTCTCACTGCGTTCA**GCAACATCCCGTGATAGCCGTATCCTCCCTCATTGCCGTCCAGTGTTTGCCTATTGGCCC**TCCTGTGCTACCGAATCT-3'
Aptamer 21 (Apta 21)	5'ATGGTCTCACTGCGTTCA**CAAGCGGTCCACGATGTGTCGCCCAATTCCCCGAACTCCGCCCGCCATGTACGTATCTCC**TCCTGTGCTACCGAATCT-3'
Aptamer 42 (Apta 42)	5'ATGGTCTCACTGCGTTCA**CACGTTGCTCATTACTCGATTGTCCTTGACGAACTCCCGTCATCCTGCCTACACCGTGCC**TCCTGTGCTACCGAATCT-3'
Aptamer 99 (Apta 99)	5'ATGGTCTCACTGCGTTCA**GCAGACATGATTGCGGAGCGATTCTCGTACTTCTGCGCCTTGTATCATTCCTCCCCTGCC**TCCTGTGCTACCGAATCT-3'
Random regions of sequences are highlighted in bold	

Data obtained from the four selected aptamers regarding the number of reads, enrichment and GC content (%) are shown in Table 3. Apta 21 showed the highest enrichment value between rounds (3.8) and GC content (cytosine and guanine bases) of 57.3% compared to the other aptamers.

Table 3
Number of reads, enrichment and GC content of candidate aptamers

Aptamer	ASC Number of reads – 7th round	ASC Number of reads – 8th round	Enrichment (fold)*	FIB Number of reads – 8th round	GC content (%)**
Apta 2	100	269	2.6	57	54.2%
Apta 21	25	95	3.8	26	57.3%
Apta 42	30	78	2.6	0	53.1%
Apta 99	22	49	2.2	0	53.1%

* Ratio between the number of reads in the 8th and 7th rounds in ASC; ** GC content = percentage equivalent to the amount of cytosine and guanine bases of the oligonucleotides.

The secondary structure of candidate aptamers and scrambled aptamer were simulated using the mfold web server at 25°C (Fig. 1).

Apta 99 showed the lowest value of Gibb's free energy (-12.71 kcal/mol), followed by Apta 21 (-11.49 kcal/mol), Apta 2 (-10.49 kcal/mol) and Apta 42 (-9.00 kcal/mol).
Scrambled showed Gibb's free energy value of -24.92 kcal/mol. We based the binding characteristic on a low Gibb's free energy values and the aptamer's high thermodynamic stability, optimizing contact with the cell membrane target. Therefore, Apta 99 is the candidate aptamer with the greatest thermodynamic stability. Among the Cell-SELEX studies present in the literature, it is observed that the total ΔG values of aptamers are variable within a group of negative values [25, 26].

One of the suggested and most commonly used methods to assess aptamers' binding to cultured cells is flow cytometry [1, 27]. Although the flow cytometry assay is commonly used to assess the binding of aptamers to cultured cells, quantitative PCR validation stands out due to the reduction amount of the number of cells required for this validation assays. Besides that, aptamer binding by flow cytometry requires trypsinization or non-enzymatic dissociation of cells, which is not recommended. For adherent cells, such as ASC, the dissociation of the plastic surface can modify the conformation of proteins and other molecules in the cell membrane and, therefore, introduce a bias in the process of selection and in vitro validation of candidate aptamers.

Aptamers can be recovered by elution after incubation with the target cells, amplified by PCR and evaluated quantitatively compared to the control cells. To avoid errors in this quantification, the presence of a normalizing sequence is necessary. Thus, the AT1 sequence from the vegetable *Arabdopsis thaliana* was inserted in binding assays according to the method proposed by Graziani and colleagues [17]. Other groups and we have also demonstrated the binding of DNA aptamers and the internalization of RNA aptamers in various types of cells using qPCR [18, 24, 28, 29] opening up the possibility of future clinical application of this technique as an efficient alternative to the use of flow cytometry. The results of the binding assays are shown in Fig. 2. Box-plot graphs showed that there was no difference in binding capacity of aptamer 42 (Fig. 2c) and scrambled (Fig. 2e) when comparing ASC and FIB. We also observed that the interaction of aptamers with the molecular targets present on cells' surface occurs with more affinity than the scrambled sequence, whose interaction is nonspecific. Aptamers 2 (Fig. 2a), 21 (Fig. 2b) and 99 (Fig. 2d) showed better in vitro binding capacity to ASC compared to FIB (***$p < 0.001$).

The Kd of these three potential candidates are shown in Fig. 3. The Kd for Apta 2 incubated with ASC was 82.44 ± 4.44 nM (Fig. 3a) and, when incubated with FIB was 44.39 ± 2.14 nM (Fig. 3d). The Kd for Apta 21 incubated with ASC was 50.46 ± 2.28 nM (Fig. 3b) and 86.78 ± 9.14 nM with FIB (Fig. 3e). For Apta 99 incubated with ASC, the Kd was 72.71 ± 10.3 nM (Fig. 3c) and, when incubated with FIB was undetermined (ambiguous) (Fig. 3f).

Candidate aptamers 21 and 99 showed more affinity for ASC and less affinity for FIB, unlike aptamer 2 whose affinity was greater for fibroblasts. Considering aptamers 21 and 99, we hypothesize that both aptamers have important binding motifs to detect molecular targets present in the ASC membrane, but only Apta 99 showed specificity for the target cells since the Kd for FIB was undetermined. Although Apta 21 showed greater enrichment between rounds and higher percentages of GC content (Table 3), Apta 99 showed the lowest value of Gibb's free energy (Fig. 1), indicating better structural stability under room temperature conditions.

In recent years, studies have been conducted to identify mesenchymal stem cells derived from diverse tissues using aptamers. Ueki and colleagues [30] developed a DNA aptamer named TD0 capable of support the self-renewal and pluripotency of induced pluripotent stem cells (iPSCs). A study by Hou and collaborators [31] was important for the discovery of an aptamer called Apt19S that demonstrated a high affinity for induced pluripotent human stem cells (iPSCs), mouse embryonic stem cells (mESCs), Rhesus monkey ESCs and human embryonic stem cells (hESCs). Wang and colleagues [32] used whole-cell SELEX to generate a novel mesenchymal stem cells (MSCs) aptamer termed HM69. This aptamer was applied to functional aptamer-directed nanoparticles to recruit MSCs for bone defect regeneration. Another group developed a cartilage tissue-engineering scaffold functionalized with an aptamer (Apt19s) that specifically recognizes pluripotent stem cells [33]. Despite the literature, our data emerge as pioneers applying Cell-SELEX to identify human ASC using human dermal fibroblasts as negative selection control. This tool can be applied to isolation protocols to ensure the preparation of ASC free from other cellular contaminants, especially fibroblasts. Also, Apta 99 can bind to an extracellular marker, which allows the identification of ASC in matrix/scaffold culture systems.

4. Conclusions

In conclusion, the Cell-SELEX method has been successfully adapted to select aptamers capable of binding with more affinity and efficiency to mesenchymal stem cells derived from human adipose tissue. It was possible to identify thermodynamically stable candidate sequences and to determine the dissociation constant (Kd) of these aptamers by quantitative PCR. This technique is highly sensitive and effective, but it is not yet commonly used in aptamer validation tests. According to our results, Apta 99 was the most promising aptamer for accurate identification of ASC in future cell purification assays and cell therapy protocols.

Declarations

Funding

This study was funded by FAPEMIG (Fundação de Amparo à Pesquisa do Estado de Minas Gerais), CNPq (Conselho Nacional de Desenvolvimento Científico e Tecnológico) and CAPES (Coordenação de Aperfeiçoamento de Pessoal de Nível Superior).

Conflicts of interest/Competing interests

The authors have no conflicts of interest to declare that are relevant to the content of this article.

Ethics approval

All procedures performed in studies involving human participants were in accordance with the ethical standards of the institutional and/or national research committee and with the 1964 Helsinki Declaration and its later amendments or comparable ethical standards. The study was approved by the Research Ethics Committee of the Universidade Federal de Minas Gerais (No. 02508018.1.0000.5149).

Consent to participate

Informed consent was obtained from all individual participants included in the study.

Availability of data and material

The data that supports the findings of this study are included in this article and available in the supplementary information.

Authors' contributions

All authors contributed to the study's conception and design. Material preparation, data collection and analysis were performed by Mariane Izabella Abreu de Melo, Pricila da Silva Cunha, Marcelo Coutinho de Miranda, Joana Lobato Barbosa, Jerusa Araújo Quintão Arantes Faria and Dawidson Assis Gomes. Funding acquisition, resources and supervision were provided by Michele Angela Rodrigues, Pricila da Silva Cunha, Alfredo Miranda de Goes and Dawidson Assis Gomes. Mariane Izabella Abreu de Melo wrote the first draft of the manuscript and all authors commented on previous versions of the manuscript. All authors read and approved the final manuscript.

ORCID

Mariane Izabella Abreu de Melo https://orcid.org/0000-0001-7150-9435

Pricila da Silva Cunha https://orcid.org/0000-0001-5456-9727
Marcelo Coutinho de Miranda https://orcid.org/0000-0002-9021-4912

Jerusa Araújo Quintão Arantes Faria https://orcid.org/0000-0001-7974-0295

Michele Ângela Rodrigues https://orcid.org/0000-0002-0233-7729

Alfredo Miranda de Goes https://orcid.org/0000-0002-0262-949X

Dawidson Assis Gomes https://orcid.org/0000-0001-7714-991X

References

1. Sefah, K., Shangguan, D., Xiong, X., O'Donoghue, M. B., & Tan, W. (2010). Development of DNA aptamers using Cell-SELEX. *Nature protocols*, *5*(6), 1169–1185. https://doi.org/10.1038/nprot.2010.66
2. Tuerk, C., & Gold, L. (1990). Systematic evolution of ligands by exponential enrichment: RNA ligands to bacteriophage T4 DNA polymerase. *Science (New York, N.Y.)*, *249*(4968), 505–510. https://doi.org/10.1126/science.2200121
3. Ellington, A. D., & Szostak, J. W. (1990). In vitro selection of RNA molecules that bind specific ligands. *Nature*, *346*(6287), 818–822. https://doi.org/10.1038/346818a0
4. Quang, N. N., Miodek, A., Cibiel, A., & Ducongé, F. (2017). Selection of Aptamers Against Whole Living Cells: From Cell-SELEX to Identification of Biomarkers. *Methods in molecular biology (Clifton, N.J.), 1575*, 253–272. https://doi.org/10.1007/978-1-4939-6857-2_16
5. Zuk, P. A., Zhu, M., Ashjian, P., De Ugarte, D. A., Huang, J. I., Mizuno, H., Alfonso, Z. C., Fraser, J. K., Benhaim, P., & Hedrick, M. H. (2002). Human adipose tissue is a source of multipotent stem cells. *Molecular biology of the cell*, *13*(12), 4279–4295. https://doi.org/10.1091/mbc.e02-02-0105

6. Zuk P (2013) Adipose-Derived Stem Cells in Tissue Regeneration: A Review. Int Sch Res Not 2013:e713959. https://doi.org/10.1155/2013/713959
7. Pereira, M. C., Secco, M., Suzuki, D. E., Janjoppi, L., Rodini, C. O., Torres, L. B., Araújo, B. H., Cavalheiro, E. A., Zatz, M., & Okamoto, O. K. (2011). Contamination of mesenchymal stem-cells with fibroblasts accelerates neurodegeneration in an experimental model of Parkinson's disease. *Stem cell reviews and reports*, *7*(4), 1006–1017. https://doi.org/10.1007/s12015-011-9256-4
8. Halfon, S., Abramov, N., Grinblat, B., & Ginis, I. (2011). Markers distinguishing mesenchymal stem cells from fibroblasts are downregulated with passaging. *Stem cells and development*, *20*(1), 53–66. https://doi.org/10.1089/scd.2010.0040
9. Kundrotas, G. (2012). Surface markers distinguishing mesenchymal stem cells from fibroblastos.*Acta medica Lituanica*, 19(2), pp. 75-79. doi: 10.6001/actamedica.v19i2.2313.
10. Bourin, P., Bunnell, B. A., Casteilla, L., Dominici, M., Katz, A. J., March, K. L., Redl, H., Rubin, J. P., Yoshimura, K., & Gimble, J. M. (2013). Stromal cells from the adipose tissue-derived stromal vascular fraction and culture expanded adipose tissue-derived stromal/stem cells: a joint statement of the International Federation for Adipose Therapeutics and Science (IFATS) and the International Society for Cellular Therapy (ISCT). *Cytotherapy*, *15*(6), 641–648. https://doi.org/10.1016/j.jcyt.2013.02.006
11. Flavell, S. J., Hou, T. Z., Lax, S., Filer, A. D., Salmon, M., & Buckley, C. D. (2008). Fibroblasts as novel therapeutic targets in chronic inflammation. *British journal of pharmacology*, *153 Suppl 1*(Suppl 1), S241–S246. https://doi.org/10.1038/sj.bjp.0707487
12. Soundararajan, M., & Kannan, S. (2018). Fibroblasts and mesenchymal stem cells: Two sides of the same coin?. *Journal of cellular physiology*, *233*(12), 9099–9109. https://doi.org/10.1002/jcp.26860
13. Alt, E., Yan, Y., Gehmert, S., Song, Y. H., Altman, A., Gehmert, S., Vykoukal, D., & Bai, X. (2011). Fibroblasts share mesenchymal phenotypes with stem cells, but lack their differentiation and colony-forming potential. *Biology of the cell*, *103*(4), 197–208. https://doi.org/10.1042/BC20100117
14. Halfon, S., Abramov, N., Grinblat, B., & Ginis, I. (2011). Markers distinguishing mesenchymal stem cells from fibroblasts are downregulated with passaging. Stem cells and development, 20(1), 53–66. https://doi.org/10.1089/scd.2010.0040
15. Denu, R. A., Nemcek, S., Bloom, D. D., Goodrich, A. D., Kim, J., Mosher, D. F., & Hematti, P. (2016). Fibroblasts and Mesenchymal Stromal/Stem Cells Are Phenotypically Indistinguishable. *Acta haematologica*, *136*(2), 85–97. https://doi.org/10.1159/000445096
16. Abreu de Melo, M. I., da Silva Cunha, P., Coutinho de Miranda, M., Faraco, C., Barbosa, J. L., da Fonseca Ferreira, A., Kunrath Lima, M., Faria, J., Rodrigues, M. Â., de Goes, A. M., & Gomes, D. A. (2021). Human adipose-derived stromal/stem cells are distinct from dermal fibroblasts as evaluated by biological characterization and RNA sequencing. *Cell biochemistry and function*, 10.1002/cbf.3610. Advance online publication. https://doi.org/10.1002/cbf.3610
17. Graziani, A.C., Stets, M.I,, Lopes, A.L.K, et al (2017) High efficiency binding aptamers for a wide range of bacterial sepsis agents. J Microbiol Biotechnol 27:838–843. https://doi.org/10.4014/jmb.1611.11004
18. Thiel, W. H., Bair, T., Peek, A. S., Liu, X., Dassie, J., Stockdale, K. R., Behlke, M. A., Miller, F. J., Jr, & Giangrande, P. H. (2012). Rapid identification of cell-specific, internalizing RNA aptamers with bioinformatics analyses of a cell-based aptamer selection. *PloS one*, *7*(9), e43836. https://doi.org/10.1371/journal.pone.0043836
19. Mencin, N., Šmuc, T., Vraničar, M., Mavri, J., Hren, M., Galeša, K., Krkoč, P., Ulrich, H., & Šolar, B. (2014). Optimization of SELEX: comparison of different methods for monitoring the progress of in vitro selection of aptamers. *Journal of pharmaceutical and biomedical analysis*, *91*, 151–159. https://doi.org/10.1016/j.jpba.2013.12.031
20. Thiel W. H. (2016). Galaxy Workflows for Web-based Bioinformatics Analysis of Aptamer High-throughput Sequencing Data. *Molecular therapy. Nucleic acids*, *5*(8), e345. https://doi.org/10.1038/mtna.2016.54
21. Liu, W., & Saint, D. A. (2002). A new quantitative method of real time reverse transcription polymerase chain reaction assay based on simulation of polymerase chain reaction kinetics. *Analytical biochemistry*, *302*(1), 52–59. https://doi.org/10.1006/abio.2001.5530
22. Cikos, S., Bukovská, A., & Koppel, J. (2007). Relative quantification of mRNA: comparison of methods currently used for real-time PCR data analysis. *BMC molecular biology*, *8*, 113. https://doi.org/10.1186/1471-2199-8-113
23. Pfaffl M. W. (2001). A new mathematical model for relative quantification in real-time RT-PCR. *Nucleic acids research*, *29*(9), e45. https://doi.org/10.1093/nar/29.9.e45
24. Izabella Abreu de Melo, M., Rodrigues Correa, C., da Silva Cunha, P., Miranda de Góes, A., Assis Gomes, D., & Silva Ribeiro de Andrade, A. (2020). DNA aptamers selection for carcinoembryonic antigen (CEA). *Bioorganic & medicinal chemistry letters*, *30*(15), 127278. https://doi.org/10.1016/j.bmcl.2020.127278
25. Souza, A. G., Marangoni, K., Fujimura, P. T., Alves, P. T., Silva, M. J., Bastos, V. A., Goulart, L. R., & Goulart, V. A. (2016). 3D Cell-SELEX: Development of RNA aptamers as molecular probes for PC-3 tumor cell line. *Experimental cell research*, 341(2), 147–156. https://doi.org/10.1016/j.yexcr.2016.01.015
26. Vidic, M., Smuc, T., Janez, N., Blank, M., Accetto, T., Mavri, J., Nascimento, I. C., Nery, A. A., Ulrich, H., & Lah, T. T. (2018). In Silico Selection Approach to Develop DNA Aptamers for a Stem-like Cell Subpopulation of Non-small Lung Cancer Adenocarcinoma Cell Line A549. *Radiology and oncology*, 52(2), 152–159. https://doi.org/10.2478/raon-2018-0014
27. Nascimento, I. C., Nery, A. A., Bassaneze, V., Krieger, J. E., & Ulrich, H. (2016). Applications of Aptamers in Flow and Imaging Cytometry. *Methods in molecular biology (Clifton, N.J.)*, *1380*, 127–134. https://doi.org/10.1007/978-1-4939-3197-2_10
28. Avci-Adali, M., Wilhelm, N., Perle, N., Stoll, H., Schlensak, C., & Wendel, H. P. (2013). Absolute quantification of cell-bound DNA aptamers during SELEX. *Nucleic acid therapeutics*, *23*(2), 125–130. https://doi.org/10.1089/nat.2012.0406

29. Li, H.H., Wen, C.Y., Hong, C.Y., Lai, J.C. (2017) Evaluation of aptamer specificity with or without primers using clinical samples for C-reactive protein by magnetic-assisted rapid aptamer selection. RSC Adv 7:42856–42865. https://doi.org/10.1039/c7ra07249j
30. Ueki, R., , Atsuta, S., , Ueki, A., , Hoshiyama, J., , Li, J., , Hayashi, Y., , & Sando, S., (2019). DNA aptamer assemblies as fibroblast growth factor mimics and their application in stem cell culture. *Chemical communications (Cambridge, England)*, *55*(18), 2672–2675. https://doi.org/10.1039/c8cc08080a
31. Hou, Z., Meyer, S., Propson, N. E., Nie, J., Jiang, P., Stewart, R., & Thomson, J. A. (2015). Characterization and target identification of a DNA aptamer that labels pluripotent stem cells. *Cell research*, *25*(3), 390–393. https://doi.org/10.1038/cr.2015.7
32. Wang, M., Wu, H., Li, Q., Yang, Y., Che, F., Wang, G., & Zhang, L. (2019). Novel Aptamer-Functionalized Nanoparticles Enhances Bone Defect Repair By Improving Stem Cell Recruitment. *International journal of nanomedicine*, *14*, 8707–8724. https://doi.org/10.2147/IJN.S223164
33. Wang, X., Song, X., Li, T., Chen, J., Cheng, G., Yang, L., & Chen, C. (2019). Aptamer-Functionalized Bioscaffold Enhances Cartilage Repair by Improving Stem Cell Recruitment in Osteochondral Defects of Rabbit Knees. *The American Journal of Sports Medicine*, *47*(10), 2316–2326. https://doi.org/10.1177/0363546519856355

Figures

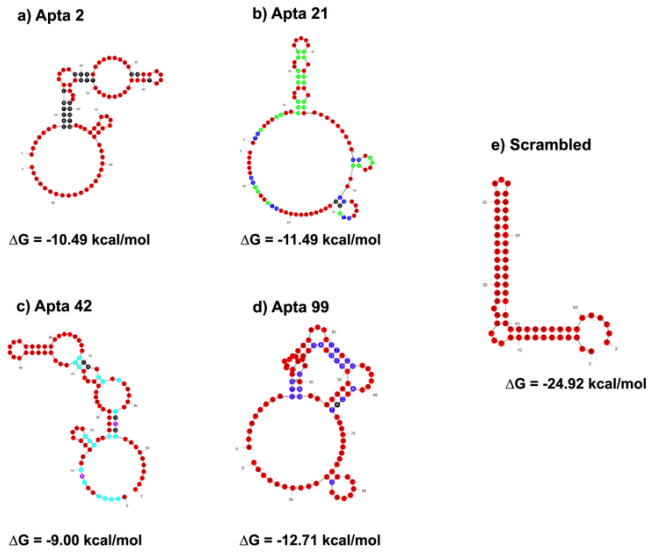

Figure 1

Predicted secondary structures of four aptamers selected for in vitro analyses. The structural predictions and ΔG values of (a) Apta 2, (b) Apta 21, (c) Apta 42, (d) Apta 99 and (e) Scrambled were obtained using the mfold web server, including the primer regions under 25°C

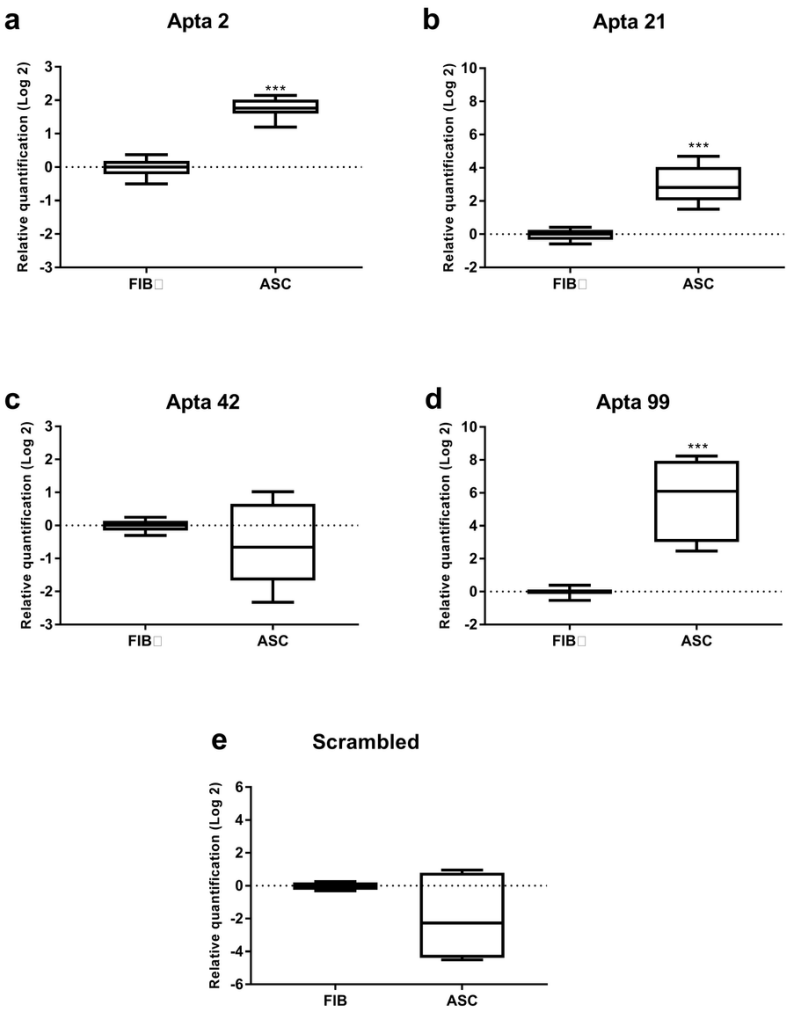

Figure 2

Apta 2, 21 and 99 shows higher binding capacity to ASC compared to FIB. (a) Binding capacity of Apta 2 to ASC compared to FIB (Mean= -0.59, SD= ±1.18). (b) Binding capacity of Apta 21 to ASC compared to FIB (Mean= 1.77, SD= ±0.29). (c) Binding capacity of Apta 42 to ASC compared to FIB (Mean= 2.97, SD= ±1.08). (d) Binding capacity of Apta 99 to ASC compared to FIB (Mean= 5.65, SD= ±2.28). (e) Binding capacity of scrambled to ASC compared to FIB (Mean= -1.94, SD= ±2.67). Unpaired t-test with Welch's correction; ***p < 0.0001; n =3

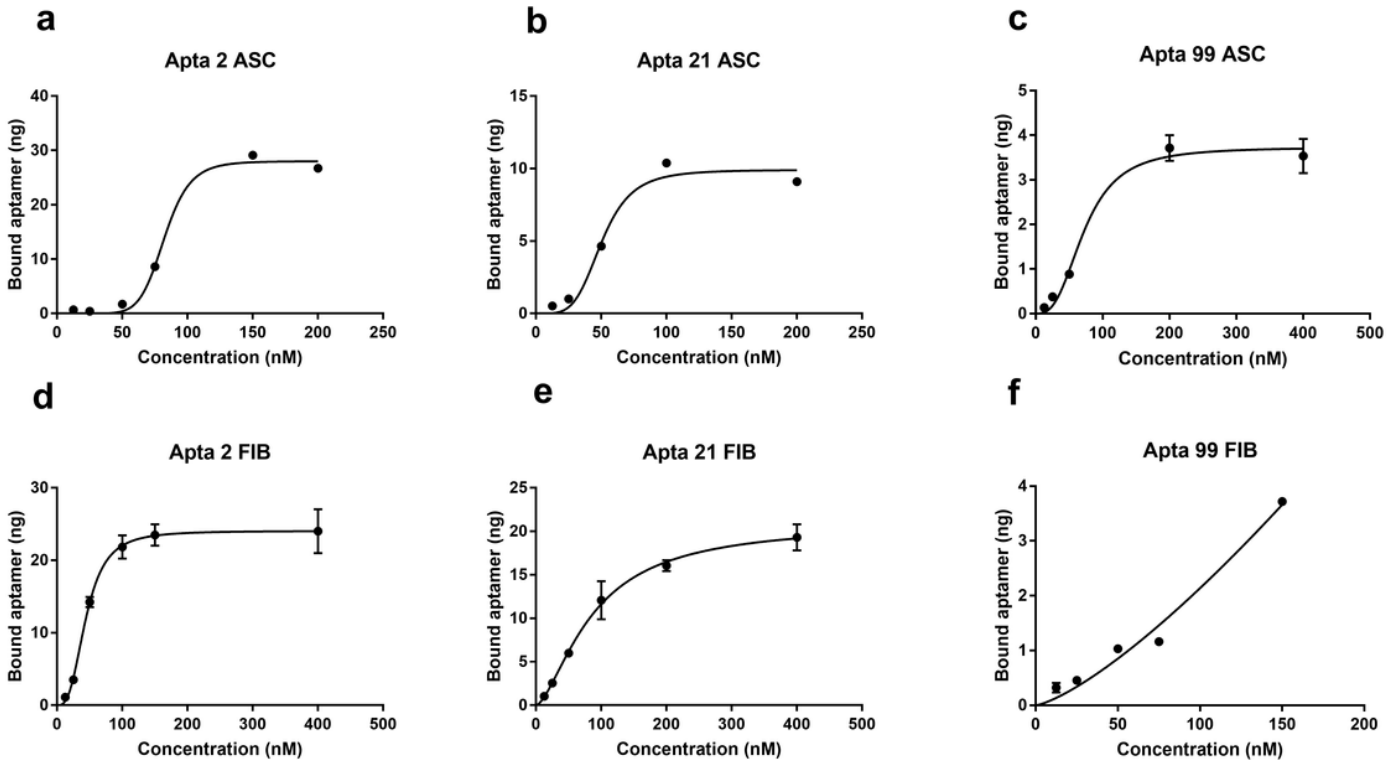

Figure 3

Apta 99 showed binding specificity to ASC compared to FIB. Kd was calculated using the specific binding with Hill slope equation. (a) The Kd for Apta 2 incubated with ASC was 82.44 ± 4.44 nM with R2 = 0.99. (b) The Kd for Apta 21 incubated with ASC was 50.46 ± 2.28 nM with R2 = 0.97. (c) The Kd for Apta 99 incubated with ASC was 72.71 ± 10.3 nM with R2 = 0.98. (d) The Kd for Apta 2 incubated with FIB was 44.39 ± 2.14 nM with R2 = 0.98. (e) The Kd for Apta 21 incubated with FIB was 86.78 ± 9.14 nM with R2 = 0.98. (f) The Kd for Apta 99 incubated with FIB was undetermined (ambiguous) with R2 = 0.97; n=3

Supplementary Files

This is a list of supplementary files associated with this preprint. Click to download.

- SupplementaryInformationFigS1.tif